Molecular Cell, Volume *32*

Supplemental Data

AKAP-Lbc Mobilizes a Cardiac Hypertrophy Signaling Pathway

Graeme K. Carnegie, Joseph Soughayer, F. Donelson Smith, Benjamin S. Pedroja, Fang Zhang, Dario Diviani, Michael R. Bristow, Maya T. Kunkel, Alexandra C. Newton, Lorene K. Langeberg, and John D. Scott

SUPPLEMENTAL EXPERIMENTAL PROCEDURES

Antibodies and Reagents

Anti-alpha-actinin (mouse monoclonal, 1:1000), anti-tubulin (mouse monoclonal, 1:5000), anti-FLAG-M2 (mouse monoclonal, 1:5000) and anti-FLAG-agarose conjugate were from Sigma-Aldrich. Anti-HDAC5 and PKD/PKCmu (and anti-phospho-PKD-Ser744/748) (rabbit polyclonal; 1:1000) were from Cell Signaling Technology. Anti-atrial natriuretic peptide (ANF; mouse monoclonal) was from US Biological. Anti-14-3-3 was from Santa Cruz (mouse monoclonal, 1:1000). Forskolin, phenylephrine, phorbol 12,13-dibutyrate (PDBu), 3-isobutyl-1-methylxanthine (IBMX), Go 6976 and microcystin-LR were from Calbiochem (San Diego, CA). Endothelin-1, isoproterenol and KN93 were from Sigma. Calyculin A was from Upstate.

RT-PCR

Total RNA was extracted from cultured cardiomyocytes (and heart tissue samples) using TRIzol reagent (Invitrogen) according to the manufacturer's instructions. 5 μg total RNA was used in each reaction for reverse transcription PCR, using the SuperScript III First-Strand Synthesis System (Invitrogen). Complementary DNAs (cDNAs) were synthesized by two distinct methods; one with oligo dT primers, the second using random hexamer

primers. cDNA was pooled and then treated with RNase to remove any RNA. The cDNA was then analyzed for specific gene expression by quantitative real-time PCR using the Platinum SYBR green qPCR SuperMix-UDG (Invitrogen). PCR conditions used to amplify all genes were as follows: 50^0C for 2 min, 95^0C for 2 min. 45 cycles of: 95^0C for 15 sec, 55^0C for 30 sec and 72^0C for 30 sec. Specificity of the SYBR green assays was confirmed by melting-point analysis and gel electrophoresis of the PCR products. Negative control reactions were also performed with the RNA used for RT-PCR to confirm there was no contamination of genomic DNA. Real-time PCR reactions were performed, recorded, and analyzed using a Stratagene Mx3000P cycler. Expression data were calculated from the cycle threshold (Ct) value using the $\Delta\Delta$Ct method for quantification (Bustin et al., 2005). Gene expression of GAPDH was used for normalization.

Amplification was performed by using the following primers:

rat ANP: 5'-ATCTGATGGATTTCAAGAACC-3' (forward) and

5'-CTCTGAGACGGGTTGACTTC-3' (reverse)

human ANP: 5'-ACCTGATGGATTTCAAGAATT-3' (forward) and

5'-CTCTGGGCTGGGCTGACTTC-3' (reverse)

rat GAPDH: 5'-AGCCCAGGATGCCCTTTAGT-3' (forward) and

5'-AGCCCAGGATGCCCTTTAGT-3' (reverse)

human GAPDH: 5'- GGTCGGAGTCAACGGATTTG-3' (forward) and

5'-CGGTGCCATGGAATTTGCC-3' (reverse)

rat α-actinin: 5'-CCTGCTGTTGGACCCGGC-3' (forward) and

5'-GGAAGTCCTCATCGATGTTC-3' (reverse)

human α-actinin: 5'-CCTGCTCCTGGACCCAGC-3' (forward) and

5'-TGAAGTCTTCCTCGATGTTC-3' (reverse)

rat AKAP-Lbc: 5’-GGTCAATGAGTCAACAGAATCC-3’ (forward) and

5’-GGCTCCATGACTCTGCTTC-3’ (reverse)

human Lbc: 5'-GGATGTGAATTCCCTTGATAAGAAG-3’ (forward) and

5’-CCACGTCAACCTCAGCAGTCC-3’ (reverse).

Expression constructs

The cDNA for wild type GFP-tagged PKD was provided by Dr. Vivek Malhotra (UCSD). PKD was HA- and GST-tagged using the Gateway cloning system (Invitrogen), as described previously (Carnegie et al., 2004). AKAP-Lbc constructs were expressed with a YFP and FLAG tag using the pEYFP-N1 vector (Clontech). GST-AKAP-Lbc fusion proteins were produced in BL21(DE3)pLys (Carnegie et al., 2004). Equivalent N-terminal-Myc-tagged-AKAP-Lbc fragments were cloned into pDEST12-myc using the Gateway cloning system (Invitrogen) for expression in HEK293 cells. Rat AKAP-Lbc shRNA and human AKAP-Lbc (control) shRNA was provided by Dr. Dario Diviani (Univ. Lausanne, Switzerland) and is described in Appert-Coline et al., 2007.

Plasmids encoding HDAC5 and Mef2-luciferase were provided by Dr. Eric Olson (UTSW). HDAC5 vector was subsequently modified for the expression of HDAC5 protein with a Cerulean or Red fluorescent protein tag. In addition HDAC5 was cloned into pcDNA3.1D/V5-His-TOPO (Invitrogen) for expression with a V5 epitope-tag. Plasmid encoding FLAG-14-3-3γ was provided by Dr. Tony Pawson (Samuel Lunenfeld Institute, Toronto, Canada). Plasmid encoding DKAR was kindly provided by Dr. Alexandra Newton (UCSD). Nuclear DKAR was constructed by digesting DKAR with KpnI and XbaI, the resulting fragment was used for PCR to replace the stop codon at the end of

the YFP coding sequence with a nuclear localisation coding sequence (coding for amino acid residues: pkkkrveda). This fragment was then re-ligated to form nuclear DKAR (nDKAR).

In vitro HDAC5 phosphorylation and 14-3-3 binding assays

HDAC5 immunocomplexes were phosphorylated *in vitro* in kinase assay buffer (25 mM Tris, pH 7.5, 0.1mM EGTA, 0.1mM Na_3VO_4, 0.03% Brij-35, 50 mM $MgCl_2$/0.5mM ATP) supplemented with PKD or PKA C-subunit (~0.2 μg) for 20 minutes at 30°C. Reactions were terminated by washing five times with fresh immunoprecipitation buffer prior to resuspension in 2X Laemmli sample buffer and SDS-PAGE. For binding reactions, samples were processed as follows. Immunocomplexes were phosphorylated as indicated above or were dephosphorylated for 30 minutes at 30°C using 400 U λ phosphatase (New England Biolabs) in phosphatase buffer (50 mM Tris, pH 7.5, 0.1 mM EDTA, 5 mM DTT, 0.01% Brij 35, 2 mM $MnCl_2$). After phosphorylation or dephosphorylation, complexes were washed 4X in IP buffer and then incubated in 1 ml of HEK293 lysate expressing FLAG-14-3-3γ. Samples were incubated for 1 hour at 4°C. Complexes were washed 4X in 1 ml lysis/IP buffer, resuspended in SDS sample buffer, separated by SDS-PAGE and subjected to Western blot.

Mef2-luciferase assays

Cos7 cells were seeded in 6-well dishes at a density of 3.5 x 10^4 cells per ml (1ml added per 6-well dish). Cells were transfected (the same day using Effectene (Qiagen), as described per manufacturers protocol) with plasmids for the expression of AKAP-Lbc and/or PKD in addition to the Mef2 luciferase reporter and a control β-galactosidase reporter. 16 hrs post transfection cells were treated with 50 nM phorbol ester (PDBu). Six hours after PDBu treatment cells were then harvested and the resulting lysates

assayed for luciferase and β-galactosidase activity, described as follows. Cells were harvested in 250 μl luciferase assay buffer (100 mM $NaPO_4$ pH 8.0, 4mM ATP, 1mM Na pyrophosphate, 6mM MgCl, 1μM DTT, 0.2% Triton X-100) and clarified. 50 μl lysate was used per luciferase assay (made up to a total volume of 300 μl with luciferase assay buffer without Triton) and 10 μl per β-galactosidase assay (made up to a total volume of 100 μl with β-galactosidase assay buffer; 100 mM $NaPO_4$ pH 8.0, 2mM MgCl, 0.01% Galacton Plus and incubated for 1 hour). Luciferase activity was measured using an AutoLumat LB953 tube luminometer (Berthoid), with a 100 μl injection of luciferin (1 mM) and a 30 second measurement period. β-galactosidase activity was measured with a 100 μl injection of Emerald assay buffer (250 μl Emerald II enhancer, 0.18N NaOH) and a 10 second measurement period.

All assays were carried out in triplicate. Results presented indicate average Mef2 transcriptional activity normalized to control β-galactosidase activity. Remaining lysate was used to determine even protein expression across the different conditions in several independent experiments. Parallel experiments were also carried out where cells were harvested in RIPA buffer. Lysates were used for Western blotting to confirm similar protein expression whether cells were harvested in RIPA buffer or Luciferase assay buffer.

Supplemental Reference

Bustin, S. A., Mueller, R. (2005). Clin Sci (Lond). 109(4):365-79.
Real-time reverse transcription PCR (qRT-PCR) and its potential use in clinical diagnosis.

Supplementary figure 1

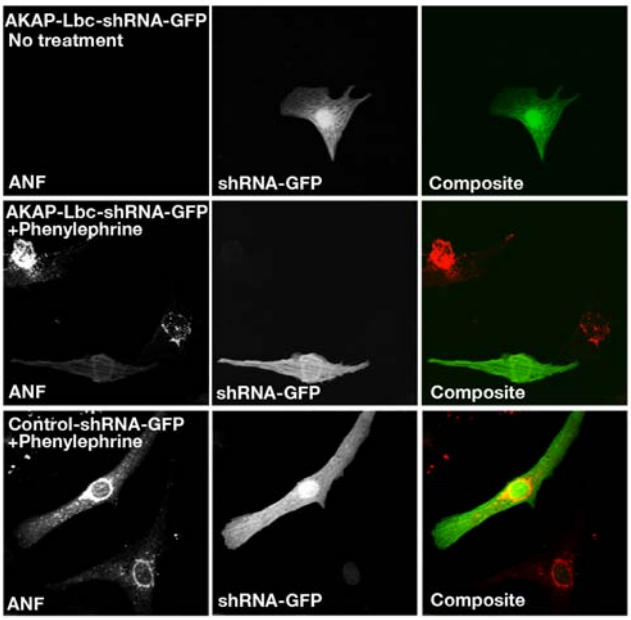

S1. shRNA-silencing of AKAP-Lbc blunts Atrial Natriuretic Factor (ANF) expression in response to phenylephrine (PE). Immunostaining for the hypertrophic marker ANF (red). RNV expressing AKAP-Lbc shRNA or cells expressing control shRNA were identified by GFP fluorescence (green). Untreated RNV do not express the hypertrophic marker ANF (top panel). Upon treatment with PE, ANF expression is observed in control cells (bottom panel) but is barely detectable in AKAP-Lbc silenced cells (middle panel).

Supplementary figure 2

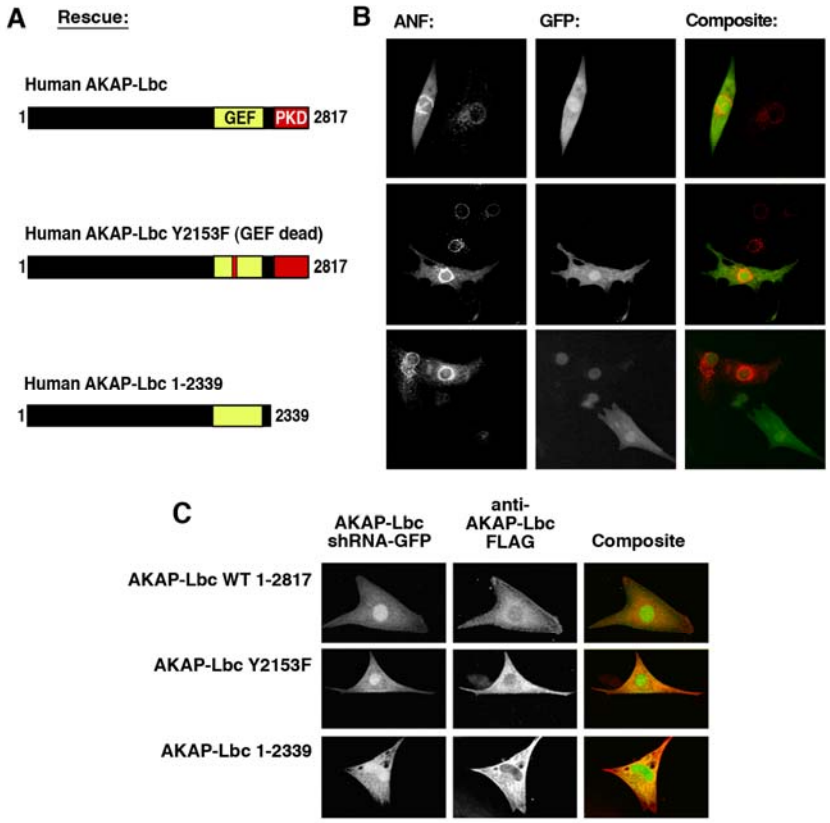

S2. RNAi rescue experiments using human AKAP-Lbc constructs in RNV. **A)** Schematic diagram of human AKAP-Lbc constructs used to rescue the anchoring protein shRNA phenotype: hAKAP-Lbc, hAKAP-Lbc-Y2153F (a guanine exchange factor (GEF)-dead mutant), AKAP-Lbc 1-2339 (C-terminal truncation mutant that is unable to bind PKD; Supplemental data S3). **B)** Full-length AKAP-Lbc is required for complete induction of ANF expression in response to PE. Immunostaining for the hypertrophic marker ANF (red). RNV expressing AKAP-Lbc shRNA were identified by GFP fluorescence (green). Upon treatment with PE, ANF expression is observed in control cells expressing human full length AKAP-Lbc in addition to rat AKAP-Lbc shRNA (top panel). PE induced ANF expression is also observed in cells expressing hAKAP-Lbc-Y2153F in addition to rat AKAP-Lbc shRNA (top panel) but is barely detectable in AKAP-Lbc silenced cells rescued with hAKAP-Lbc 1-2339 (bottom panel). **C)** RNV expressing AKAP-Lbc shRNA/GFP were detected by green fluorescence. Co-expression of rescue constructs was verified using anti-FLAG primary and Texas-Red conjugated secondary antibody.

Supplementary Figure 3

PKD binding region of AKAP-Lbc

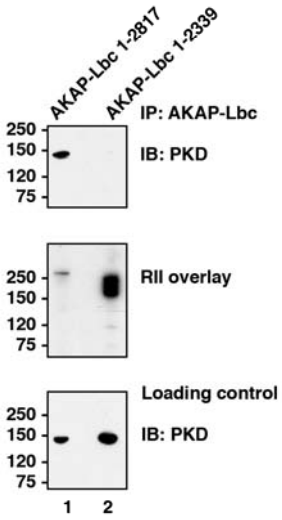

S3. PKD cannot bind to AKAP-Lbc 1-2339. Co-immunoprecipitation of AKAP-Lbc with PKD. FLAG-tagged AKAP-Lbc was immunoprecipitated from HEK293 cell lysates expressing PKD and either full-length AKAP-Lbc (1-2817) or truncated AKAP-Lbc 1-2339). Top, immunoblot detection of PKD co-immunoprecipitating with AKAP-Lbc (1-2817). Bottom, immunoblot detection of PKD from lysate. Middle, RII overlay detecting immunoprecipitated AKAP-Lbc.

Supplementary figure 4

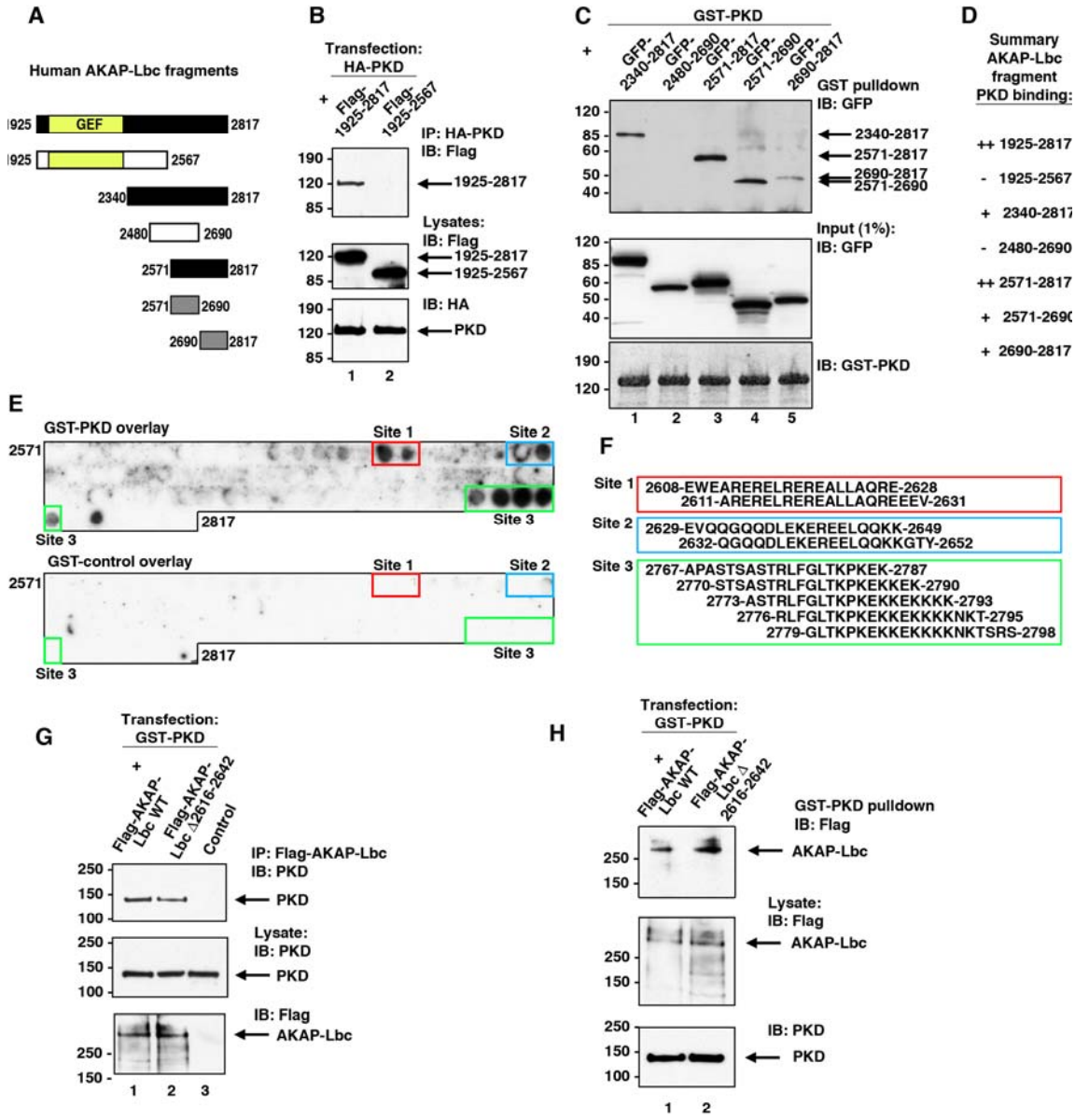

S4. Further mapping of PKD binding region in AKAP-Lbc. A) Diagram of AKAP-Lbc C-terminal fragments used for mapping studies. **B)** AKAP-Lbc 1925-2567 does not co-immunoprecipitate with PKD. HA-tagged PKD was immunoprecipitated from HEK293 cell lysates expressing HA-PKD and FLAG-AKAP-Lbc fragments. Top, immunoblot detection of AKAP-Lbc fragments co-immunoprecipitating with PKD. Bottom, immunoblot of immunoprecipitated PKD. Middle, detection of AKAP-Lbc fragments from cell lysates. **C)** Further mapping of PKD binding to AKAP-Lbc C-terminus. GST-PKD pulldowns were carried out using cell lysates expressing GST-PKD and GFP-AKAP-Lbc fragments. Top, immunoblot detection of AKAP-Lbc fragments pulled-down with PKD. Bottom, immunoblot of GST-PKD pulldown. Middle, detection of AKAP-Lbc fragments from cell lysates. **D)** Summary of data presented in A-C regarding AKAP-Lbc fragment interaction with PKD. **E)** Autospot peptide array mapping of PKD binding to AKAP-Lbc C-terminus. 20-mer peptides encompassing the C terminus of AKAP-Lbc from amino acid residues 2571-2817 were arrayed onto a membrane for overlay with GST-PKD. Top panel shows three regions of PKD binding. Bottom panel shows a GST-control overlay. **F)** Sites 1-3 encompass AKAP-Lbc peptides where PKD binding was observed **G)** PKD co-immunoprecipitates with AKAP-Lbc Δ 2616-2642. FLAG-tagged AKAP-Lbc was immunoprecipitated from HEK293 cell lysates expressing GST-PKD and FLAG-AKAP-Lbc. Top, immunoblot detection of PKD co-immunoprecipitating with AKAP-Lbc. Bottom, immunoblot of immunoprecipitated AKAP-Lbc. Middle, detection of PKD from cell lysates **H)** AKAP-Lbc Δ 2616-2642 interacts with PKD. GST-PKD was purified from HEK293 cell lysates expressing GST-PKD and FLAG-AKAP-Lbc. Top, immunoblot detection of AKAP-Lbc in GST-PKD pulldown. Bottom, immunoblot of GST-PKD in pulldown. Middle, detection of AKAP-Lbc from cell lysates.

Supplementary figure 5

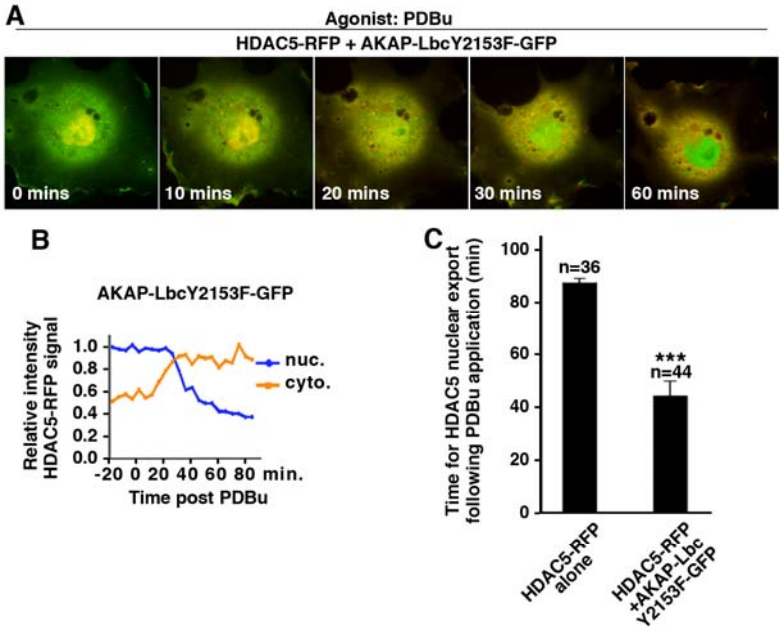

S5. Live-cell imaging to monitor the nuclear export of HDAC5-RFP in Cos7 cells co-expressing AKAP-Lbc-Y2153F-GFP.
A) PDBu was applied to Cos7 cells at 0 mins and images were collected at designated times (indicated in each frame). **B)** Relative nuclear and cytoplasmic intensity of HDAC5-RFP signal in a single representative cell. Quantitation carried out using NIH Image J software.
C) Amalgamated data from control and AKAP-Lbc Y2153F expressing cells (n=number of cells analyzed) indicating the time of HDAC5 nuclear export in Cos7 cells following application of PDBu. Data are expressed as mean +/- standard error of the mean. Differences in quantitative variables were examined by one-way analysis of variance (ANOVA) using the software InStat. A P value < 0.05 was considered significant (*), a P value < 0.01 was considered very significant (**) and a P value < 0.001 was considered extremely significant (***).

Supplementary figure 6

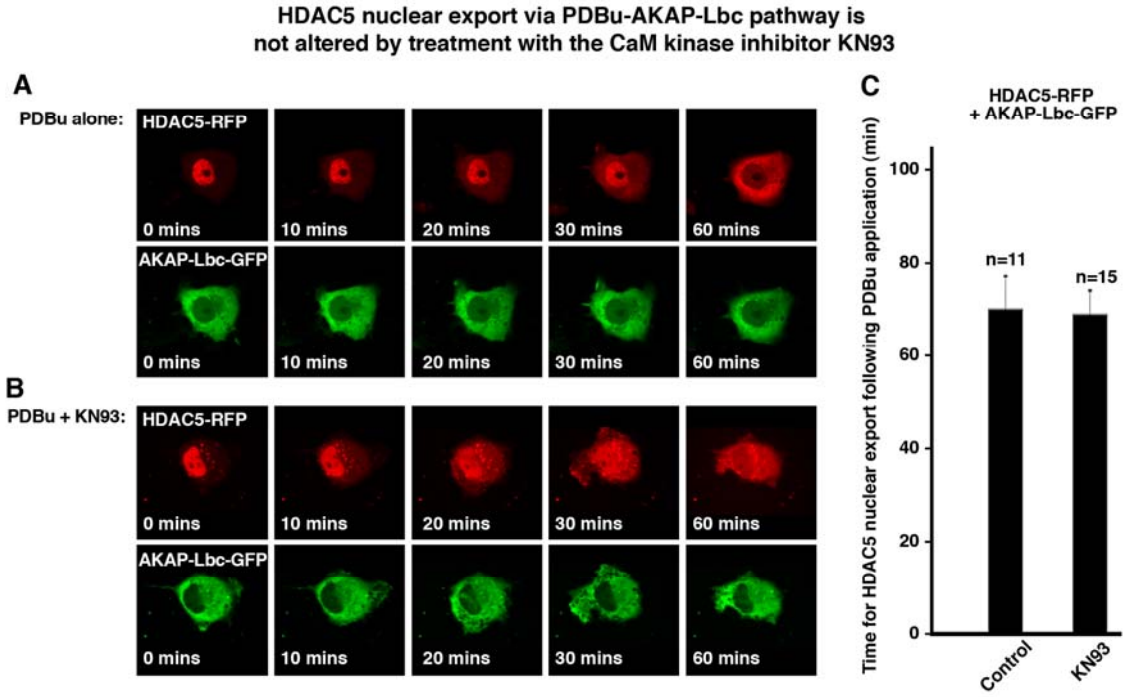

S6. CaMK inhibition does not affect AKAP-Lbc-mediated HDAC5 nuclear export in response to PDBu in Cos7 cells.
A) Nuclear export of HDAC5-RFP was monitored in Cos7 cells co-expressing AKAP-Lbc-GFP. Cells were preincubated for 20 mins. with KN93 (5 μM) prior to application of PDBu (at 0 mins). Images were collected at designated times (indicated in each frame).
B) Amalgamated data indicating the time of AKAP-Lbc mediated HDAC5 nuclear export in Cos7 cells treated with PDBu and KN93. Data are expressed as mean +/- standard error of the mean. Differences in quantitative variables were examined by one-way analysis of variance (ANOVA) using the software InStat. A P value < 0.05 was considered significant (*), a P value < 0.01 was considered very significant (**) and a P value < 0.001 was considered extremely significant (***).

Supplementary figure 7

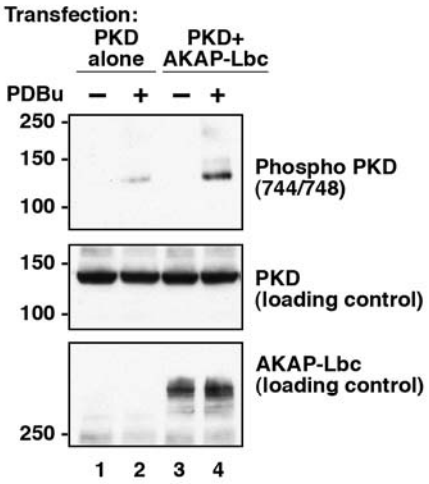

S7. AKAP-Lbc enhances phorbol ester-mediated activation of PKD. HEK293 cells expressing PKD alone or co-expressing PKD with AKAP-Lbc were untreated or stimulated with PDBu prior to lysis. Proteins were separated by SDS-PAGE. PKD activation was assessed by immunoblot using anti-phospho-Ser-744/748 PKD antibodies (top panel). Loading controls for total PKD (middle panel) and AKAP-Lbc (bottom panel) are presented.

Supplementary figure 8

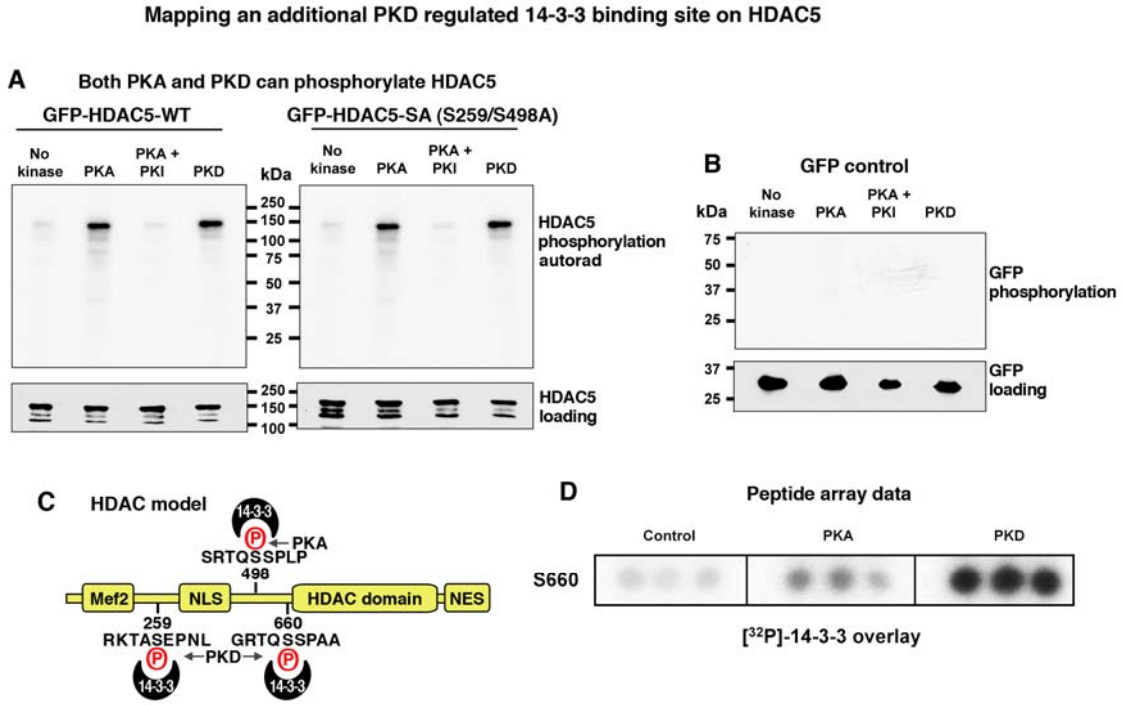

S8. Phosphorylation of HDAC5 by PKA and PKD. A) GFP-tagged-HDAC5 or a GFP-HDAC5-S259/498A double mutant were immuno-precipitated from HEK293 cells and used for an in vitro phosphorylation reaction with [32P]-γ-ATP and either purified PKA or PKD, or no kinase. Phosphorylation of HDAC5 was assessed by autoradiograph (top panels). Equal loading of HDAC5 under each condition was assessed by Western blot (bottom panels). **B)** Control experiment to examine GFP phosphorylation. Top panel shows the autoradiograph demonstrating no 32P incorporation into GFP, indicating no phosphorylation of GFP by PKA or PKD. **C)** Diagram of phosphorylation sites that regulate 14-3-3 binding on HDAC5. Consensus 14-3-3 binding sites are denoted. Kinase phosphorylation sites are indicated. **D)** Autospot peptide array data confirming that PKD phosphorylation of S660 in HDAC5 can induce 14-3-3 binding. 20-mer peptides encompassing the putative PKD-mediated 14-3-3 binding site (S660 of HDAC5) were arrayed in triplicate onto a membrane for in vitro phosphorylation and subsequent overlay by [32P]-GST-14-3-3.

Supplementary figure 9

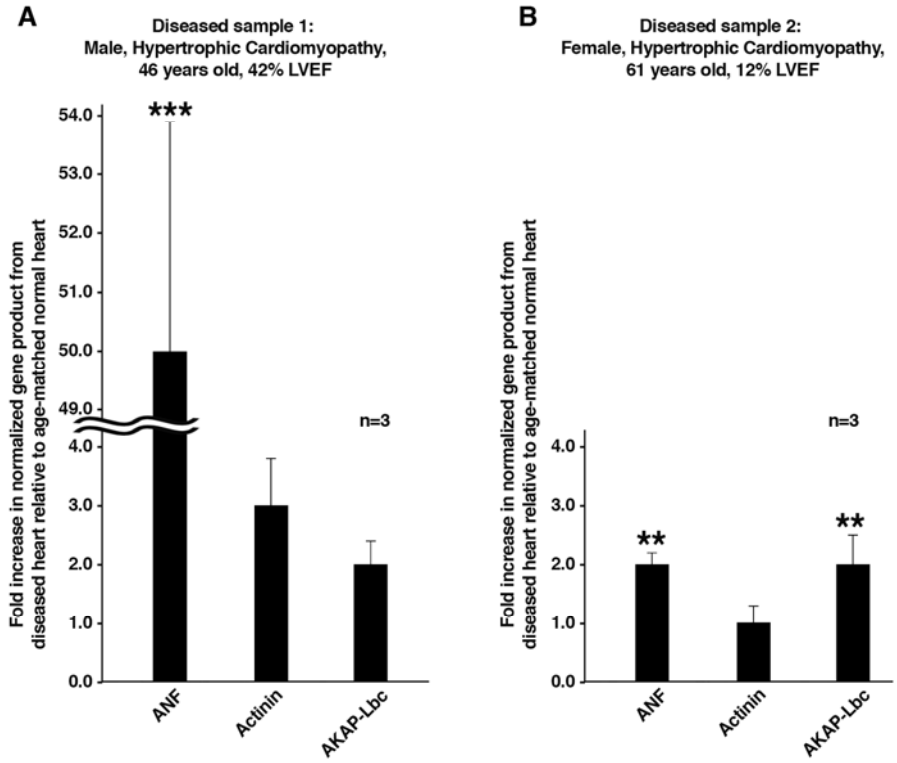

S9. AKAP-Lbc is elevated in human diseased heart. RT-PCR analysis of gene expression from RNA prepared from human diseased heart samples. Extraction of RNA from heart tissue was carried out using TriZol according to the Invitrogen protocol. RT-PCR was carried out as described in methods. Gene expression data was normalized to GAPDH gene expression. In addition to AKAP-Lbc, gene expression was examined for hypertrophic markers ANF and α-actinin. Results presented indicate the fold increase in gene product from diseased heart sample relative to that in age-matched normal heart sample. Two diseased heart samples were analyzed. Diseased sample #1 was from a 46 yr old male who exhibited hypertrophic cardiomyopathy with a 42% Left Ventricle Ejection Fraction (LVEF). The age-matched normal heart sample was from a 44 yr old male. Diseased sample #2 was from a 61 yr old female who exhibited hypertrophic cardiomyopathy with a 12% Left Ventricle Ejection Fraction (LVEF). The age-matched normal heart sample was from a 62 yr old female. Data are expressed as mean +/- standard error of the mean. Differences in quantitative variables were examined by one-way analysis of variance (ANOVA), or an unpaired two-tailed t test. A P value < 0.05 was considered significant (*), a P value < 0.01 was considered very significant (**) and a P value < 0.001 was considered extremely significant (***). All analyses were performed using InStat.

Human heart tissue samples were obtained from the UCHSC human heart tissue bank in collaboration with Michael Bristow.

Supplementary figure 10

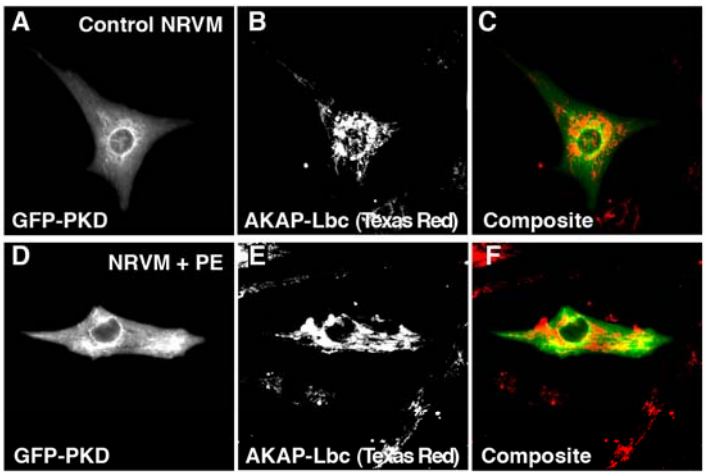

S10. Co-distribution of AKAP-Lbc and PKD in NRVM. Immunostaining of AKAP-Lbc (red) and imaging of GFP-PKD1 (green) showing subcellular localization of proteins in control cells **(A-C)** and in cells treated for 48 hrs with PE **(D-F)**.

Supplementary figure 11. Summary of HDAC5 nuclear export.

Cell type	Protein expressed	Agonist Treatment	Mean time of HDAC5 nuclear export (mins)	Number of cells analysed	Figure
Cos7	RFP-HDAC5 alone	PDBu	81 ± 7	36	3D
	RFP-HDAC5 + GFP-AKAP-Lbc	PDBu	42 ± 5	41	3D
	RFP-HDAC5 + GFP-AKAP-Lbc 1-2339	PDBu	67 ± 9	32	3D
	RFP-HDAC5 alone	PDBu	87 ± 2	36	S5
	RFP-HDAC5 + GFP-AKAP-Lbc Y2153F	PDBu	44 ± 6	44	S5
	RFP-HDAC5 alone	PDBu	66 ± 6	12	4B
	RFP-HDAC5 + YFP-AKAP-Lbc	PDBu	33 ± 3	21	4B
NRVM					
	RFP-HDAC5 alone	ET-1	53 ± 4	35	4D
	RFP-HDAC5 + YFP-AKAP-Lbc	ET-1	35 ± 5	21	4D
	RFP-HDAC5 + GFP-shRNA control	ET-1	53 ± 8	14	4F
	RFP-HDAC5 + GFP-shRNA for AKAP-Lbc	ET-1	75 ± 5	13	4F